



**Class:**  
ECE 493/593  
Section A

Project Report

**Submitted to:**  
Dr. Scott

**Submitted by:**  
Sonny Grooms  
Dhruv Birla

**Date:**  
December 08, 2023

**Table of Contents**

Introduction.....	3
Background.....	3
Theory of Operation.....	9
Analysis.....	9
Experimental Results.....	15
Discussion.....	21
Summary.....	22
Appendices.....	25

## Introduction

When designing any power electronics circuit, it is necessary to have an understanding of the losses in the system. One common source of loss in a system is switching devices, such as MOSFETs. In an ideal scenario, a MOSFET would switch on and off instantaneously with zero power loss. In reality, MOSFETs experience delays in response to turning on/off which causes them to consume power during this transition. In order to properly take this loss into account, the efficiency of the MOSFET must be quantified. This can be done through the double pulse test (DPT). A double pulse test is a standard method that uses two pulses (hence double pulse) in order to test turn on/off and reverse recovery characteristics of a MOSFET. In order to gain a better understanding of this test and switching characteristics of MOSFETs, a custom PCB was built to implement a double pulse test circuit. Depending on the configuration of the load and the inductance, this PCB can also function as a boost converter. This paper outlines the process of constructing the PCB from design to implementation, the theory of operation for a double pulse test circuit, a comparison of theoretical to measured results for both the DPT and the boost converter test, and a reflection on the project and its outcomes. Ultimately, the measured results of the double pulse test at  $I_D = 5\text{ A}$  and  $I_D = 10\text{ A}$  showed an energy loss of  $8.725$  and  $36.88\text{ }\mu\text{J}$  respectively on the MOSFET. The theoretical calculations showed that the energy loss values would be around  $9$  and  $18\text{ }\mu\text{J}$  respectively. Additionally, measurements from the boost converter set showed that the circuit was  $84.97\%$  efficient, compared to the theoretical  $85.33\%$  efficiency calculated from the overall power losses from the diode and MOSFET on the PCB.

## Background

One of the goals of this project was to gain familiarity with the process of designing and constructing a custom PCB. This meant that the first step in this project was to design the custom double pulse test PCB. Using Altium and the circuits in Figures 1, 2 and 3 below, we designed the most compact circuit possible. This was limited by the necessity to keep the low and high voltage portions of the circuit well-separated as well as the MOSFET and diode far from the control portion of the circuit but still close to each other. Having these two components too close to the low voltage components could cause EMI disturbances in them and hinder their performance. Even this early on in the design process, safety concerns were still present. When laying out the PCB for this circuit, emphasis was put on the thickness of the traces when compared to their current carrying capacity. Failure to properly size the traces could cause them to evaporate during testing under high currents which puts the PCB at risk of catching fire. The final PCB design is shown in Figure 4.

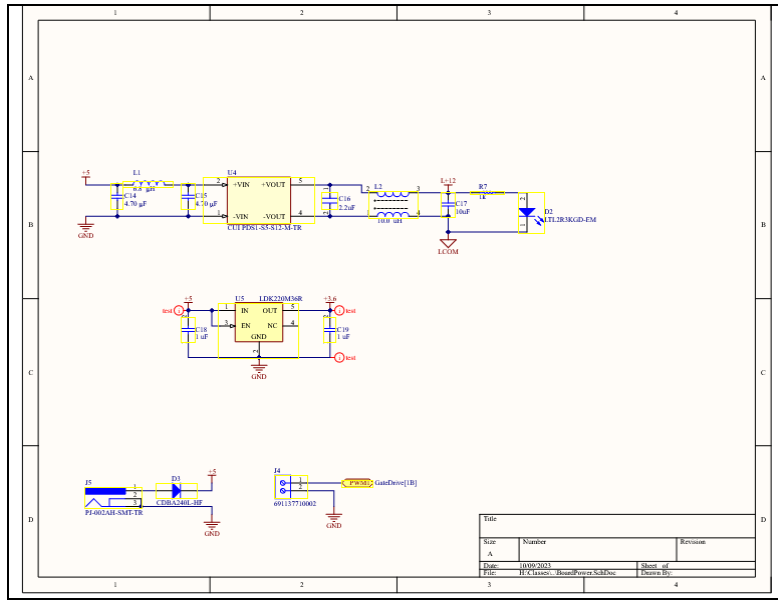


Figure 1: 5-12 V DC/DC Converter and Linear Regulator Schematic.

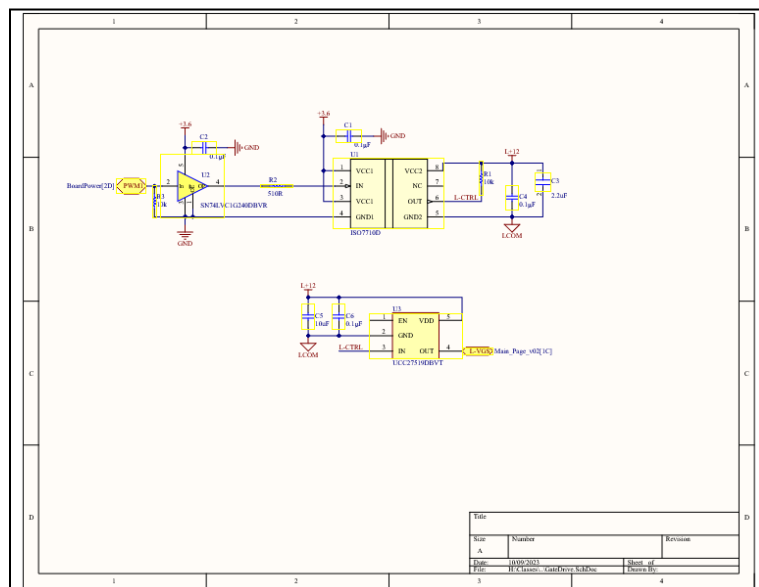


Figure 2: Digital Isolator and MOSFET Gate-drive Schematic.

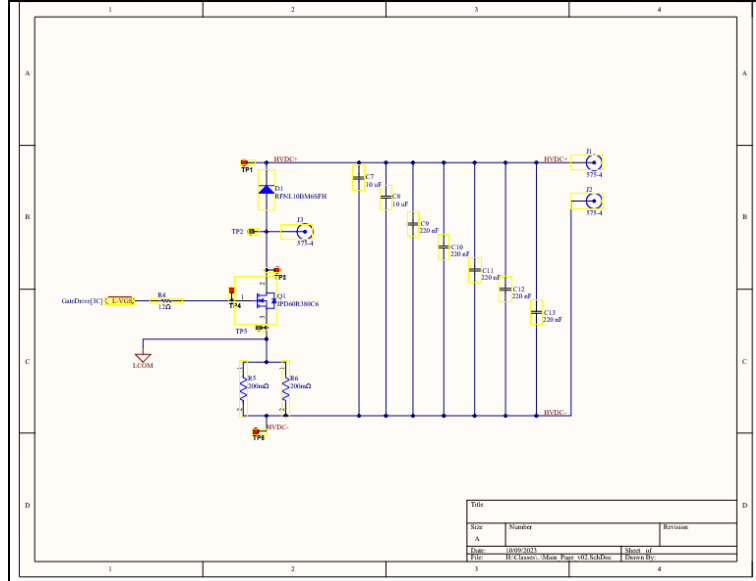


Figure 3: DPT and Low-pass Circuit Schematic.

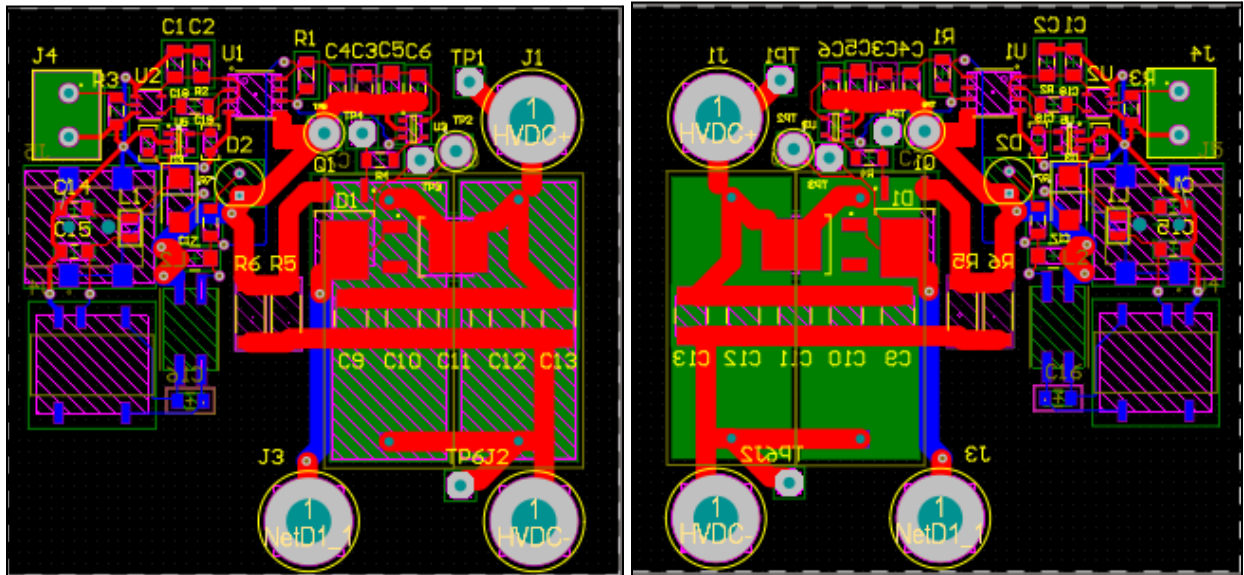


Figure 4: Final PCB Layout (from left to right: top and bottom)

Once the PCB was designed, ordered and delivered, it was time to assemble the circuit. This PCB uses mostly surface mount parts, which have the benefit of being more compact but are also much more difficult to hand-solder. In large scale production, a reflow oven is used to solder many surface mount parts at once with solder paste. This greatly reduces assembly time and increases precision while soldering. This PCB utilizes several very small components and integrated circuits that would be difficult to hand solder so it would be beneficial to be able to use a reflow oven. Rather than spending several hundred or even thousand dollars on a reflow oven, a common toaster oven was modified to accomplish the same task [1]. The modified circuit diagram is shown below in Figure 5, with the lightbulb replaced by the toaster oven and the potentiometer replaced by a thermocouple.

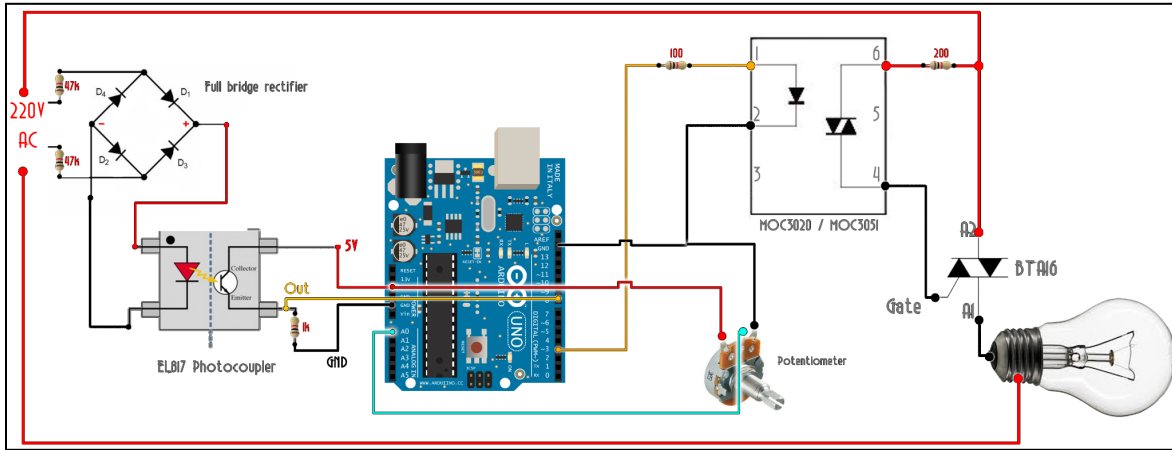


Figure 5: Unmodified circuit diagram of the reflow oven that was built to solder the components on the PCB for this project [1].

Figures 6 and 7 show the modified toaster oven and the control circuit respectively. This circuit works by taking in  $120 V_{\text{RMS}}$  and 20 A from a standard wall outlet which is split between a TRIAC and a full-bridge rectifier. The rectified signal is put into an optocoupler which converts into down to 5 VDC so that the Arduino can analyze it. The Arduino uses this signal to monitor when zero crossings occur so that it can properly time switching the TRIAC on and off. The Arduino also monitors the internal temperature inside of the oven using a type k-thermocouple rated for high temperatures. The Arduino uses this data to track the temperature of the oven over time and calculate its rate of change ( $^{\circ}\text{C}/\text{second}$ ). In order to properly melt and bond solder paste, a reflow oven must heat in a specific pattern called a reflow profile.

Figure 8 shows the reflow profile for the brand of solder paste that was used, Kester EP256. To follow this profile, the Arduino maintains a rate of change of  $2 ^{\circ}\text{C}$  per second until the oven reaches  $150 ^{\circ}\text{C}$ . Once it reaches this point, the slope is reduced to  $0.5 ^{\circ}\text{C}$  per second until a temperature of  $185 ^{\circ}\text{C}$  is reached. The oven then heats at a rate of  $3 ^{\circ}\text{C}$  per second to its peak temperature of between  $210$  and  $215 ^{\circ}\text{C}$  and maintains this for about 45 seconds. After this, the oven turns off and the PCB cools until the solder is properly set.



Figure 6: Modified Toaster Reflow Oven.

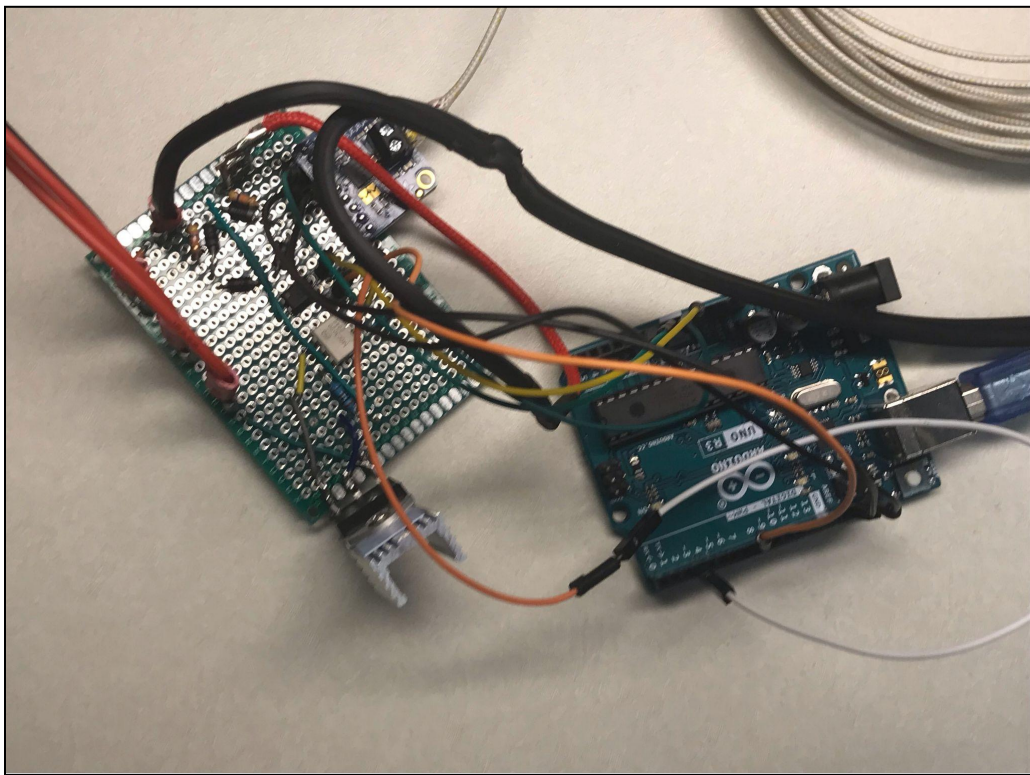


Figure 7: Oven control Circuit and Arduino Controller.

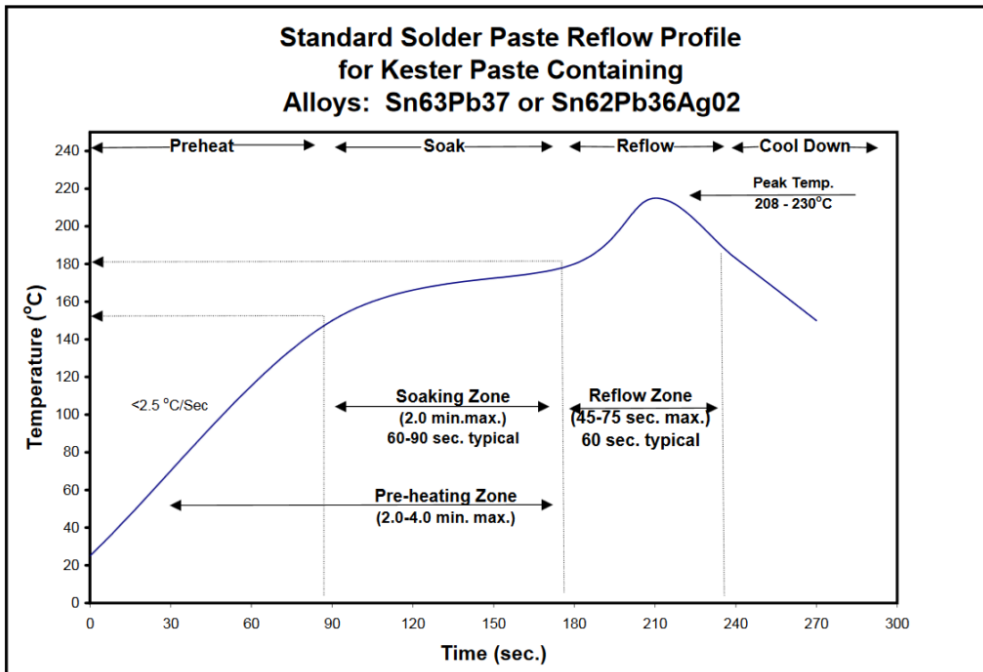


Figure 8: Kester EP256 Reflow Profile.

Figures 9 and 10 show the results of the assembly process. Aside from slight bridging on some of the smaller contacts due to excess solder paste, the oven successfully baked the board. The items on the underside of the board had to be hand soldered due to the risk of them detaching from the board during the heating process. All of the components that might not hold up well under high heat - for example, the green LED and the PWM screw connector - were also hand-soldered. The screw terminal and led had to be hand soldered as well due to them not being able to withstand the oven's high temperatures. During both the reflow process and the process of hand soldering, extreme attention to safety was kept due to the possibility of burns or inhaling toxic fumes. A ventilation fan was kept running at all times during both processes to filter any fumes and a fire extinguisher was kept on hand during the testing and running of the reflow oven. Also, during hand soldering, PCB clamps were used to hold the board firmly in place and reduce the possibility of burning someone holding the board.

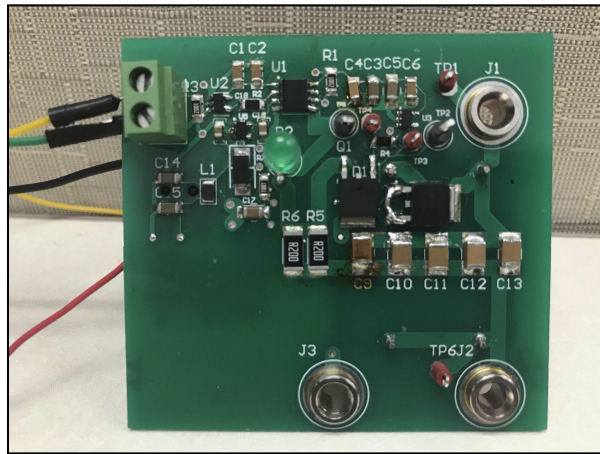


Figure 9: Top Side of PCB after Assembly

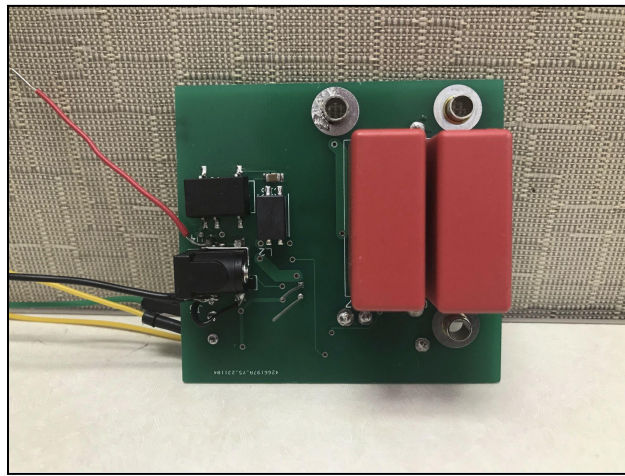


Figure 10: Bottom Side of PCB after Assembly

## Theory of Operation

The completed PCB can operate in two separate modes, both as a double pulse test and as a boost converter. This board utilizes three different inputs in order to perform these different operations. Referring to the schematics in Figures 1, 2 and 3, the first of these is a barrel jack input that takes in a 5 VDC source through a wall adapter. The 5 V is supplied to two separate ICs, the PDS1-S5-S12-M-TR (U4) and the LDK220M36R (U5). The PDS1-S5-S12-M-TR is a DC-DC converter that takes in a 5 V source and converts it to a 12 V source. This 12 V signal is used to power the UCC27519DBVT (U3) which is a gate drive used to control the IPD60R380C6 MOSFET (Q1) in the circuit and the ISO7710D (U1). Going back to the 5 V level, the LDK220M36R outputs 3.6 V which is fed to both the SN74LVC1G240DBVR (U2) and the ISO7710D. The SN74LVC1G240DBVR is an inverter that takes in a PWM signal from the second input source, the screw terminals on the board, and sends the inverted output to the ISO7710D as well. The ISO7710D is a digital isolator that takes in the inverted PWM as well 3.6 and 12 V and outputs a control signal to the UCC27519DBVT gate drive so that the low voltage portion of the circuit can control the high voltage portion. Lastly, plugs J1, J2 and J3 are used for high voltage input and output, with the output being controlled by the IPD60R380C6 MOSFET.

Both the double pulse test and boost converter modes require specific setups. Referring to Figure 4, in boost mode, a load (a variable resistor) is connected across pins J1 and J2 and a large inductor is connected between the J3 socket and a DC power supply. A 5 V input source is provided by a barrel socket on the bottom of the board. By supplying a PWM signal to J4, the output voltage can be modulated by adjusting the duty cycle. In the double pulse test configuration, the inductor is connected between the J1 and J3 sockets and the DC power supply is connected to sockets J1 and J2. The J4 screw terminal with the PWM signal and the 5 volt input socket remain connected as well. Scoping the board at the test points on the board during this test allows you to analyze different values pertaining to the double pulse test such as the Gate-Source voltage on the MOSFET.

## Analysis

### Double Pulse Test:

Below are the pulse width calculations for two different cases.

Case 1:  $v_{IN} = 25V$ ,  $i_D = 5 A$ ,  $L = 370\mu H$ :

$$V_L = L * \frac{di}{dt}$$

$$dt = \frac{L * di}{V_L}$$

$$dt = \frac{L * i_D}{v_{IN}}$$

$$dt = \frac{370 \mu H * 5 A}{25 V}$$

$$dt = 74 \mu s$$

Therefore, the pulse width for the double pulse test in this case is **74 μs**.

Case 2:  $v_{IN} = 25V$ ,  $i_D = 10 A$ ,  $L = 370\mu H$ :

$$V_L = L * \frac{di}{dt}$$

$$dt = \frac{L * di}{V_L}$$

$$dt = \frac{L * i_D}{v_{IN}}$$

$$dt = \frac{370 \mu H * 10 A}{25 V}$$

$$dt = 148 \mu s$$

Therefore, the pulse width for the double pulse test for this case is **148 μs**.

Below are the calculations for the energy loss during turn-on and turn-off of the power MOSFETs. First, calculating the energy losses for the first case when  $I_D = 5 A$ :

$$Energy loss = E_{ON} + E_{OFF}$$

$$P_{Q,SW} = \frac{1}{2} * V_{DS} * (I_{ON} * t_{ON} + I_{OFF} * t_{OFF}) * f_s = (E_{ON} + E_{OFF}) * f_s$$

$$E_{ON} = I_{Q,OFF} * t_{OFF} * \frac{1}{2} * V_{DS}$$

$$E_{ON} = 5 A * 119 ns * \frac{1}{2} * 25V = 7.438 \mu J$$

$$E_{OFF} = I_{Q,ON} * t_{ON} * \frac{1}{2} * V_{DS}$$

$$E_{ON} = 5 A * 25 ns * \frac{1}{2} * 25V = 1.563 \mu J$$

$$Energy loss = E_{ON} + E_{OFF} = 7.438 \mu J + 1.563 \mu J = 9 \mu J$$

Therefore, the theoretical energy loss across the power MOSFET when  $I_D = 5 A$  is **9 μJ**. Now, calculating energy losses for the case when  $I_D = 10 A$ :

$$Energy loss = E_{ON} + E_{OFF}$$

$$P_{Q,SW} = \frac{1}{2} * V_{DS} * (I_{Q,OFF} * t_{OFF} + I_{Q,ON} * t_{ON}) * f_s = (E_{ON} + E_{OFF}) * f_s$$

$$E_{ON} = \frac{1}{2} * V_{DS} * I_{Q,OFF} * t_{OFF}$$

$$E_{ON} = 10 A * 119 ns * \frac{1}{2} * 25V = 14.875 \mu J$$

$$E_{OFF} = \frac{1}{2} * V_{DS} * I_{Q,ON} * t_{ON}$$

$$E_{OFF} = 10 A * 25 ns * \frac{1}{2} * 25V = 3.125 \mu J$$

$$Energy\ loss = E_{ON} + E_{OFF} = 14.875 \mu J + 3.125 \mu J = 18 \mu J$$

Therefore, the theoretical energy loss across the power MOSFET when  $I_D = 10$  A is **18  $\mu J$** .

#### Boost Operation:

Below are our calculations for the case  $V_{IN} = 5V$ ,  $I_{OUT} = 0.5$  A,  $D = 0.6$ ,  $f_s = 40$  kHz,  $L = 370\mu H$ .

Starting out with the formula to determine overall efficiency:

$$Efficiency = \frac{P_{OUT} - P_{LOSS}}{P_{IN}} * 100\%$$

$$P_{OUT} = V_{OUT} * I_{OUT}$$

$$P_{IN} = V_{IN} * I_{IN}$$

$$V_{OUT} = \frac{V_{IN}}{1-D} = \frac{5V}{1-0.6} = 12.5V$$

$$I_{IN} = \frac{I_{OUT}}{1-D} = \frac{0.5A}{1-0.6} = 1.25A$$

Below are our calculations for the overall  $P_{LOSS}$  for the boost converter, which is equal to the power losses of the diode and the MOSFET added together.

$$P_{LOSS} = P_{D,TOT} + P_{Q,TOT}$$

Here is the total power loss calculation for the diode, which is equal to its conduction and switching losses added together:

$$P_{D,TOT} = P_{D,CON} + P_{D,SW}$$

$$P_{D,CON} = I_{D,Avg} * V_F$$

where  $I_{D,Avg} = I_{OUT,Avg} = 0.5 A$  due to charge-second balance and  $V_F = 0.75 V$  based on the datasheet.

$$P_{D,CON} = (0.5A)(0.75V) = 0.375 W$$

Now, calculating the diode's switching losses:

$$P_{D,SW} = V_D * Q_{RR} * f_s$$

$$P_{D,SW} = V_{D,OFF} * Q_{RR} * f_s$$

$$P_{D,SW} = V_{OUT} * Q_{RR} * f_s$$

$$P_{D,SW} = (12.5 V) * (350 nC) * (40 kHz) = 0.175 W$$

So, the total power loss across the diode is  $0.375 W + 0.175 W = 0.55 W$ . Now, moving onto the power loss across the MOSFET:

$$P_{Q,TOT} = P_{Q,CON} + P_{Q,SW}$$

Below are the calculations for the conduction losses from the MOSFET.

$$P_{Q,CON} = (I_{Q,RMS})^2 * R_{DS,ON}$$

$$I_{Q,RMS} = \sqrt{\frac{D}{3 * I_{Q,PP}} (I_{Q,MAX}^3 - I_{Q,MIN}^3)}$$

In this case,  $I_Q = I_L$  so  $I_{Q,RMS}$  and  $P_{Q,CON}$  can be calculated as follows:

$$I_{Q,PP} = I_{L,PP} = \frac{V_{IN} * D}{L * f_s} = \frac{5 V * 0.6}{370 \mu H * 40 kHz} = 0.203 A$$

$$I_{Q,Avg} = I_{L,Avg} = I_{IN,Avg} = \frac{I_{OUT,Avg}}{1-D} = \frac{0.5 A}{1-0.6} = 1.25 A$$

$$I_{Q,MAX} = I_{L,MAX} = I_{L,Avg} + \frac{1}{2} I_{L,PP} = 1.351 A$$

$$I_{Q,MIN} = I_{L,MIN} = I_{L,Avg} - \frac{1}{2}I_{L,PP} = 1.149 A$$

$$I_{Q,RMS} = \sqrt{\frac{0.6}{3 * 0.203 A} (1.351 A^3 - 1.149 A^3)} = 0.969 A$$

$$P_{Q,CON} = (0.969 A)^2 * 0.34 \Omega = 0.319 W$$

Now, calculating the MOSFET's switching losses:

$$P_{Q,SW} = \frac{1}{2} * V_{DS} * (I_{ON} * t_{ON} + I_{OFF} * t_{OFF}) * f_s$$

In this case,  $t_{ON} = t_{d(ON)} + t_{rise}$  and  $t_{OFF} = t_{d(OFF)} + t_{fall}$  as noted in the datasheet for this component.

$$I_{ON} = I_{L,MIN} \text{ and } I_{OFF} = I_{L,MAX}$$

$$V_{DS} = V_{OUT} = 12.5 V$$

$$P_{Q,SW} = \frac{1}{2} * (12.5 V) * (1.149 A * 25 ns + 1.351 A * 119 ns) * 40 kHz = 47.36 mW$$

The total power loss across the MOSFET is  $0.319 W + 0.04736 W = 0.36636 W$  and  $P_{LOSS} = P_{D,TOT} + P_{Q,TOT} = 0.916 W$ . With this information, the efficiency can finally be calculated:

$$Efficiency = \frac{P_{OUT} - P_{LOSS}}{P_{IN}} * 100\%$$

$$Efficiency = \frac{V_{OUT} * I_{OUT} - P_{LOSS}}{V_{IN} * I_{IN}} * 100\%$$

$$Efficiency = \frac{12.5 V * 0.5 A - 0.916 W}{5 V * 1.25 A} * 100\%$$

$$Efficiency = 85.33 \%$$

The final estimated efficiency for the boost converter is **85.33 %**.

Below are the calculations for the voltage ripple of the output capacitor, where  $C = 220 \mu F$ :

$$v_{OUT,PP} = \frac{I_{OUT} * D}{C * f_s}$$

$$v_{OUT,PP} = \frac{0.5 A * 0.6}{220 \mu F * 40 kHz} = 34.1 mV$$

Therefore, the voltage ripple of the output capacitor is **34.1 mV**.

Below are the calculations for the junction temperature of the two power devices when a heatsink is not used:

$$T_{J,D} = (P_{D,TOT} * R_{TH,JA}) + T_A$$

$$T_{J,D} = (0.55 W * 12 \frac{\circ C}{W}) + 25 \circ C = 31.6 \circ C$$

$$T_{J,Q} = (P_{Q,TOT} * R_{TH,JA}) + T_A$$

$$T_{J,Q} = (0.36636 W * 35 \frac{\circ C}{W}) + 25 \circ C = 37.8 \circ C$$

The junction temperatures of the diode and the MOSFET without a heatsink are **49.3 °C** and **37.8 °C**, respectively.

Below is the calculation for the thermal impedance required from a heatsink given that the power devices stay below 85 °C when the ambient temperature is 30 °C and  $R_{CS} = 1 \text{ }^{\circ}\text{C/W}$ . In this case, the calculations were done using the power loss across the diode since that is greater than the power loss across the MOSFET and the heatsink needs to account for the greatest thermal dissipation that will occur.

$$T_S = T_A + (P_{Q,TOT} + P_{D,TOT}) * R_{TH,SA} = 85 \circ C$$

$$T_{D,J} = P_{D,TOT} * (R_{TH,JC} + R_{TH,CS}) + T_S$$

$$T_{D,J} = 0.55 W * (4.5 \frac{\circ C}{W} + 1 \frac{\circ C}{W}) + 85 \circ C = 88.025 \circ C$$

$$R_{TH,SA} = \frac{T_{D,J} - P_{D,TOT} * (R_{TH,JC} + R_{TH,CS}) - T_A}{P_{Q,TOT} + P_{D,TOT}} = 60.02 \frac{\circ C}{W}$$

The required thermal impedance of the heatsink is calculated to be **60.02 °C/W**. One component that fits this requirement and is readily available on DigiKey is the 501100B00000G shown in Figure 11 below, which has a thermal resistance of 63 °C/W. The part is linked in Appendix B.



Figure 11: Selected 501100B00000G heatsink from DigiKey

## Experimental Results

To verify that the constructed PCB was operational, we performed both the double pulse test and boost converter operation. Images of the DPT and boost converter setups are shown below in Figures 12, 13, and 14:

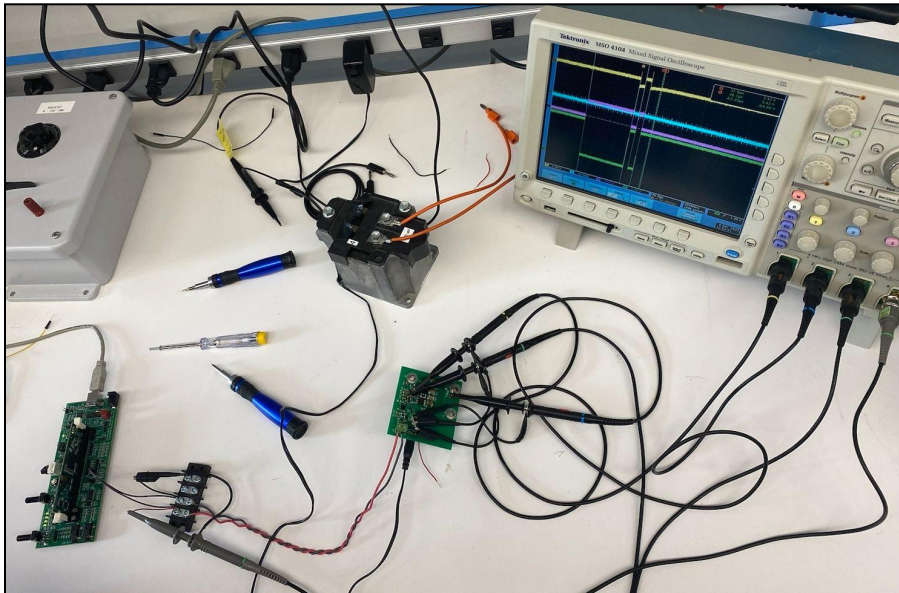


Figure 12: Image of the DPT setup. The inductor will be connected to terminals J3 and J1 of the PCB, and the power supply providing 25 VDC will connect to terminals J1 and J2 on the PCB.

Following the setup procedure outlined in the “Theory of Operation” section, the PCB was placed in the DPT configuration and the DC power supply was set to 25 V. A PWM signal was sent to the J4 screw terminal in order to switch the MOSFET. The board was then scoped at test points TP3, TP4 and TP6 as well as at the PWM input. The resulting waveforms are shown below in Figure 13. Channel 4 (green) shows the control signal supplied as the PWM signal. It consists of two pulses, one long and one short, as is the procedure for the double pulse test. Channel 3 (purple) shows the Drain-to-Source voltage of the MOSFET. It switches in response to the PWM signal which, when analyzed on a smaller time scale, provides information about the turn on and turn off time of the MOSFET. Channel 2 (blue) is the drain current of the MOSFET and Channel 1 (yellow) is  $V_{GS}$ , the former of which shows significant noise and oscillation. This is due to stray inductance which signifies deficiencies in the PCB layout.

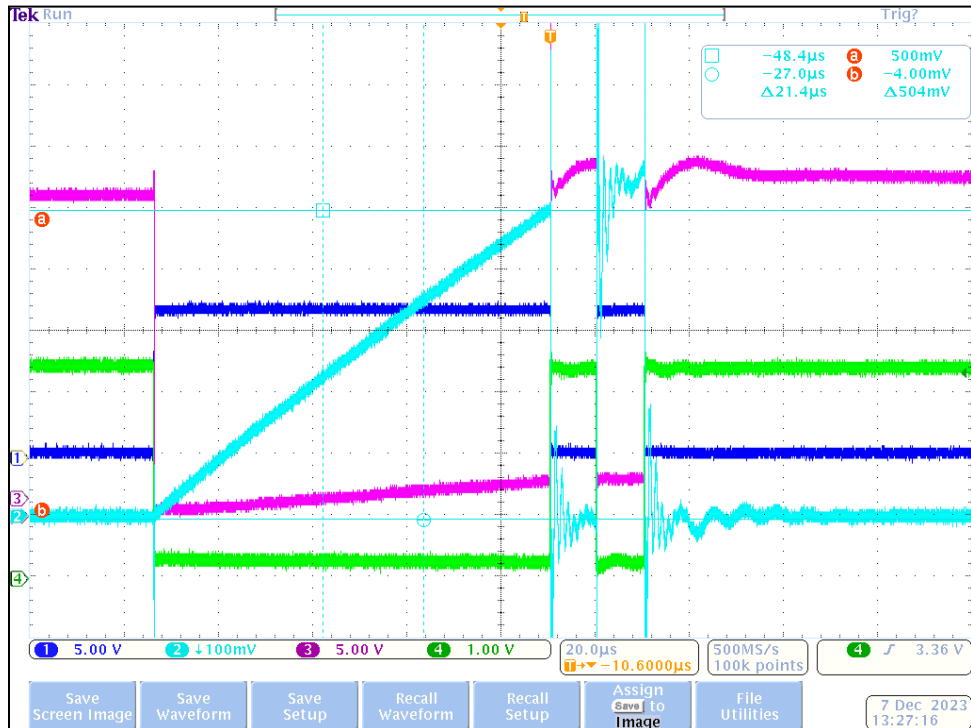


Figure 13: Sample DPT waveform from the Mixed Signal Oscilloscope

Figure 14 below shows the boost converter setup, complete with multimeters, inductor, and power supply connection to the PCB:

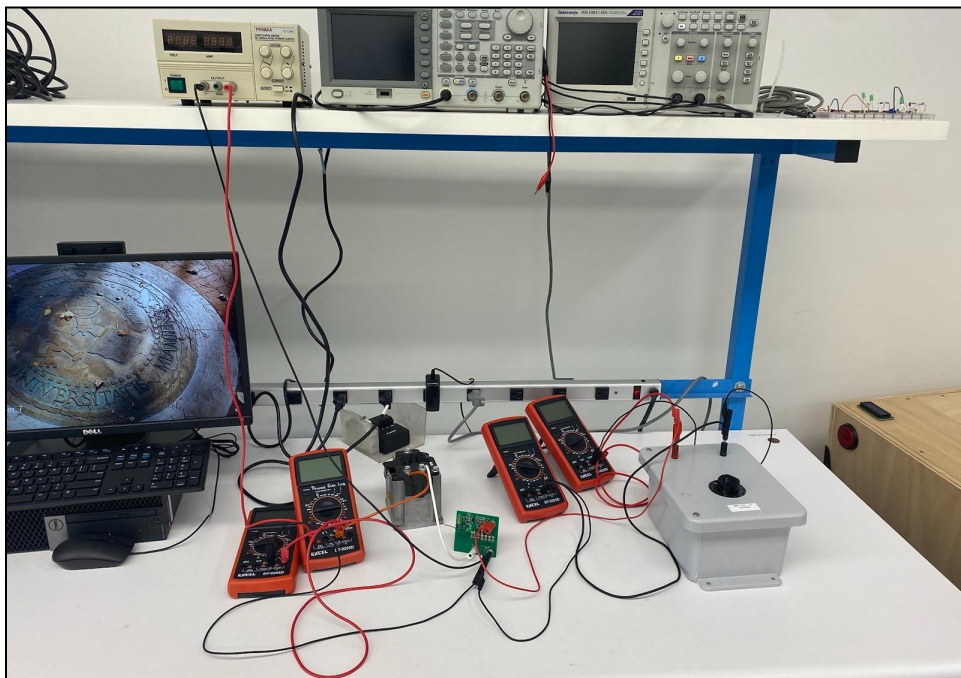


Figure 14: Image of Boost Converter Experiment with multimeters for efficiency measurements

The boost converter configuration shown above in Figure 14 was done according to the setup procedure outlined in the “Theory of Operation” section. Data is obtained in this mode of operation via four multimeters placed at the input and output of the circuit. One multimeter is placed in series with the inductor and one in series with the load in order to measure input and output current respectively. The other two multimeters are placed parallel to the inductor and load to measure the input and output voltage respectively.

## Tests

- (1) Double pulse test results at  $V_{DS} = 25V$ ,  $I_D = 5A$  and  $I_D = 10A$ .

The oscilloscope waveforms of the turn-on and turn-off event when  $I_D = 5 A$  are shown in Figures 15 and 16 below:

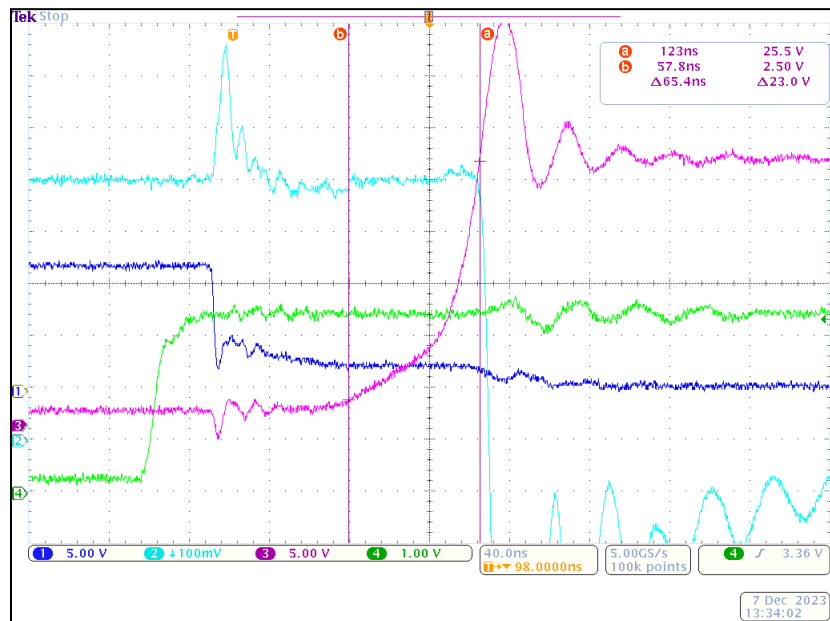


Figure 15: Measured  $t_{rv}$  (drain-source voltage rise time) using the cursors for  $I_D = 5 A$

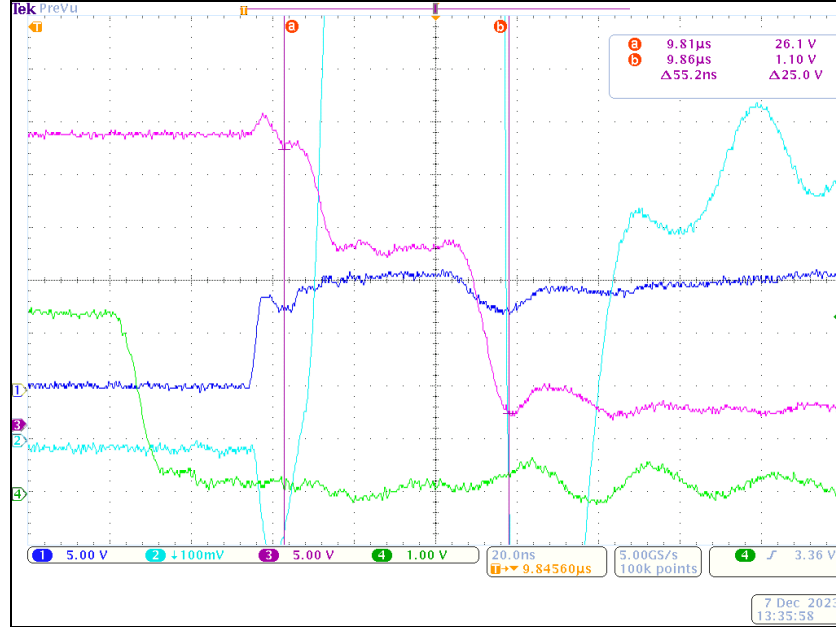


Figure 16: Measured  $t_{fv}$  (drain-source voltage fall time) using the cursors for  $I_D = 5 \text{ A}$

Based on the plots above, the values in Table I were measured for the MOSFET DPT when  $I_D = 5 \text{ A}$ . The PCB layout used in this project was very condensed, which introduced stray inductance making it difficult to obtain good measurements for  $t_{ri}$  and  $t_{fi}$ , the drain current rise and fall times respectively. Therefore, these values specifically were obtained from the datasheet.

Table I: Measured time values for DPT when  $I_D = 5 \text{ A}$

$t_{ri}$ : drain current rise time	10 ns
$t_{fv}$ : $V_{DS}$ fall time	55.2 ns
$t_{fi}$ : drain current fall time	9 ns
$t_{rv}$ : $V_{DS}$ rise time	65.4 ns

The energy consumption of the MOSFET for the  $I_D = 5 \text{ A}$  test can be derived using the switching times and the following equation:

$$\text{Energy loss} = E_{ON} + E_{OFF}$$

$$E_{ON} = \frac{1}{2} * V_{DS} * I_{Q,OFF} * t_{OFF}$$

$$E_{OFF} = \frac{1}{2} * V_{DS} * I_{Q,ON} * t_{ON}$$

$$\frac{1}{2} * V_{DS} * 5 \text{ A} * [(55.2 \text{ ns} + 10 \text{ ns}) + (65.4 \text{ ns} + 9 \text{ ns})] = 8.725 \mu\text{J}$$

Using this experimental data shows that the energy loss is **8.725 μJ** when  $I_D = 5 \text{ A}$ . The oscilloscope waveforms of the turn-on and turn-off event when  $I_D = 10 \text{ A}$  are shown in Figures 17 and 18 below:

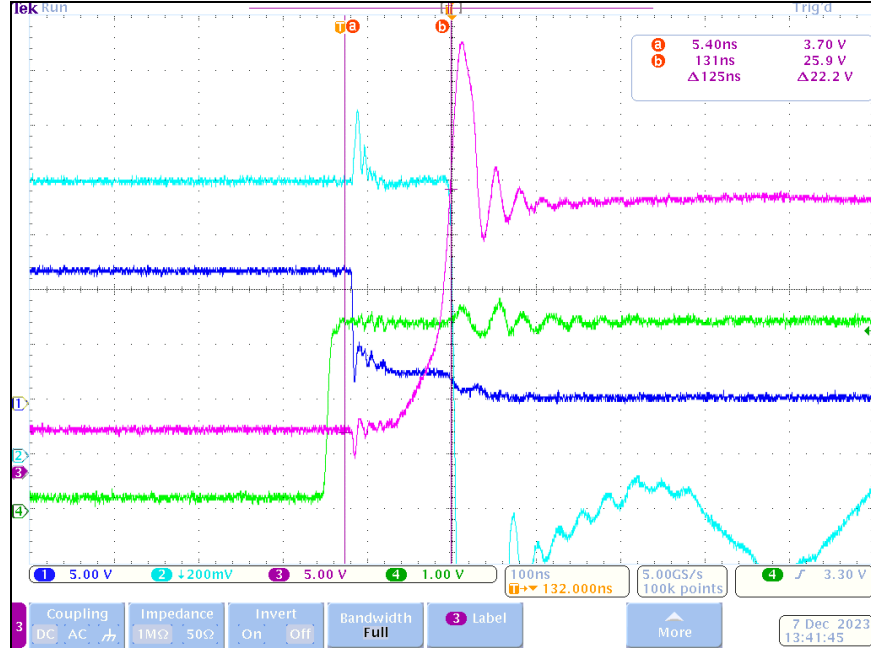


Figure 17: Measured  $t_{rv}$  (drain-source voltage rise time) using the cursors for  $I_D = 10 \text{ A}$

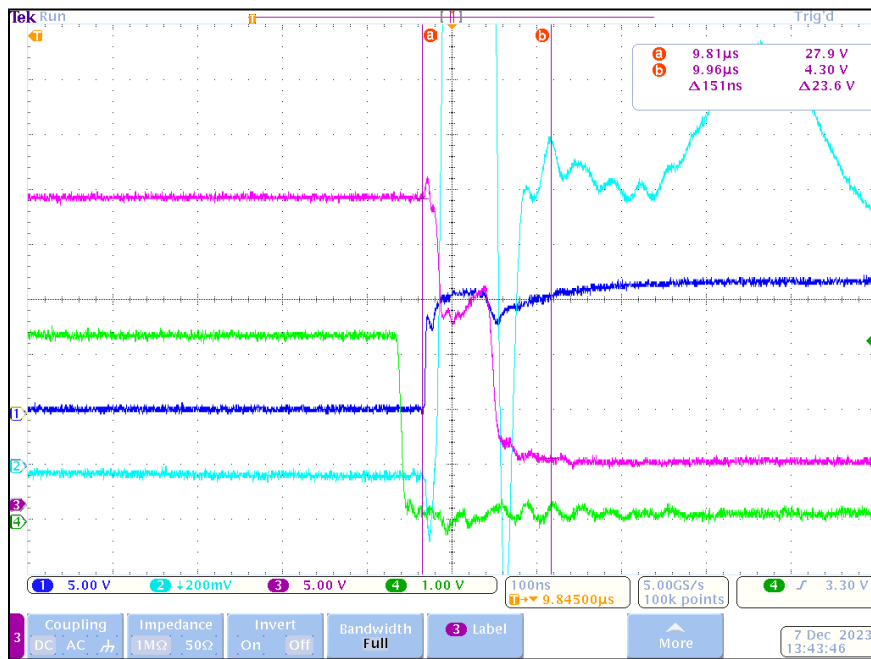


Figure 18: Measured  $t_{fv}$  (drain-source voltage fall time) using the cursors for  $I_D = 10 \text{ A}$

Based on the plots above, the values in Table II were measured for the MOSFET DPT when  $I_D = 10 \text{ A}$ . Similar to the  $I_D = 5 \text{ A}$  test, the PCB stray inductance made it difficult to obtain good measurements for  $t_{ri}$  and  $t_{fi}$ , the drain current rise and fall times respectively. These values specifically were obtained from the datasheet.

Table II: Measured time values for DPT when  $I_D = 10 \text{ A}$

$t_{ri}$ : drain current rise time	10 ns
$t_{fv}$ : $V_{DS}$ fall time	151 ns
$t_{fi}$ : drain current fall time	9 ns
$t_{rv}$ : $V_{DS}$ rise time	125 ns

The energy consumption of the MOSFET can be derived using the switching times and the following equation:

$$\text{Energy loss} = E_{ON} + E_{OFF}$$

$$E_{ON} = \frac{1}{2} * V_{DS} * I_{Q,OFF} * t_{OFF}$$

$$E_{OFF} = \frac{1}{2} * V_{DS} * I_{Q,ON} * t_{ON}$$

$$\frac{1}{2} * V_{DS} * 10 \text{ A} * [(151 \text{ ns} + 10 \text{ ns}) + (125 \text{ ns} + 9 \text{ ns})] = 36.88 \mu\text{J}$$

Using this experimental data shows that the energy loss is **36.88  $\mu\text{J}$**  when  $I_D = 10 \text{ A}$ , higher than the theoretical value of 18  $\mu\text{J}$  calculated earlier. This can be attributed to excessive stray inductance in the PCB layout as mentioned earlier. Also, the theoretical calculations assume operation in an ideal situation, and real-world tests hardly ever meet the requirements for an ideal test if at all.

The waveform on channel 2 in Figure 13 shows a voltage of around 504 mV on the diode. From the schematic in Figure 3, the shunt resistance across which this voltage is being measured is 100  $\text{m}\Omega$ . This brings the diode peak-to-peak current to about 5.04 A. This value can be used to derive the validate inductor value through the following equation:

$$V_L = L * \frac{di}{dt}$$

$$L = V_L * \frac{dt}{di}$$

$$(25 \text{ V}) * \frac{80 \mu\text{s}}{5.04 \text{ A}} = 396.8 \mu\text{H}$$

The calculated inductance of **396.8  $\mu$ H** is very close to the actual value, 370  $\mu$ H, that was used during the DPT.

- (2) Efficiency measurements for boost converter operating at  $V_{IN} = 5V$ ,  $I_{OUT} = 0.5 A$ ,  $D = 0.6$ ,  $f_s = 40 \text{ kHz}$ ,  $L = 370\text{uH}$ .

The test setup was conducted for  $I_{IN} = 0.5 A$  rather than  $I_{OUT} = 0.5 A$ , but the efficiency measurements can still be calculated accurately. The measurements are shown below in Figure 19. Below are the calculations from those results:

$$\text{Efficiency} = \frac{P_{OUT}}{P_{IN}} * 100\%$$

$$\text{Efficiency} = \frac{V_{OUT} * I_{OUT}}{V_{IN} * I_{IN}} * 100\% = \frac{7.12 V * 0.29 A}{4.86 V * 0.50 A} * 100\% = 84.97\%$$

The calculated efficiency for the boost converter comes out to **84.97%**, which is right under the theoretical efficiency of 85.33% calculated previously.

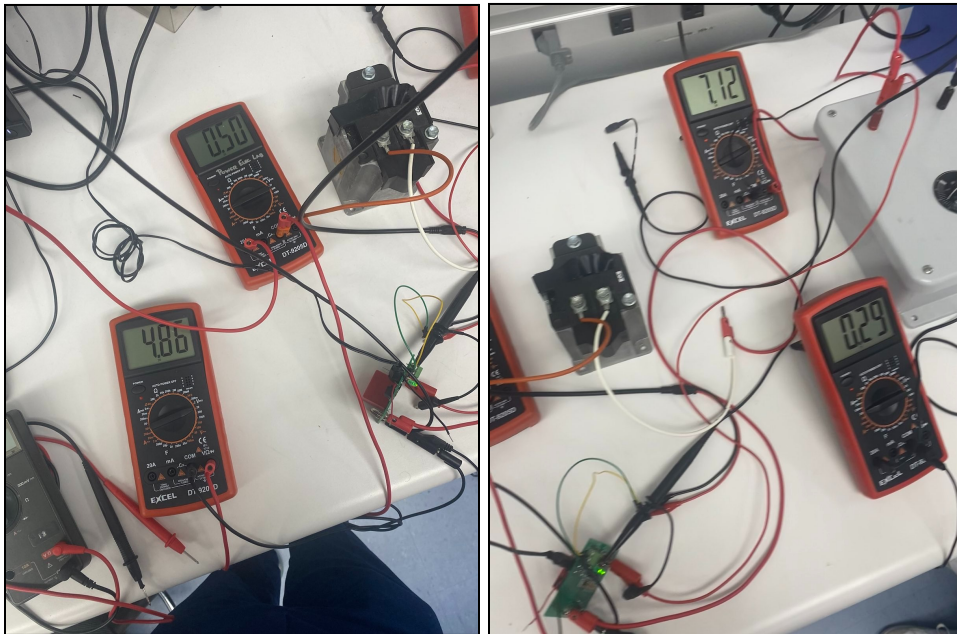


Figure 19: Efficiency measurements for the boost converter test showing input voltage and current measurements (left) and output voltage and current measurements (right).

## Discussion

Comparing the results of the double pulse test with the theoretical calculations performed, it is easy to see the necessity for understanding the actual losses of MOSFETs. Although values for  $t_{ri}$  and  $t_{fi}$  were derived from the datasheet and not the experiments, comparing  $t_{rv}$  and  $t_{fv}$  shows that the system is significantly more lossy than the theoretical system. The theoretical  $t_{ON}$  and  $t_{OFF}$  for the MOSFET is 10 ns and 9 ns respectively.  $t_{ON}$  is equal to the

sum of  $t_{rv}$  and  $t_{d(ON)}$  while  $t_{OFF}$  is equal to the sum of the  $t_{ri}$  and  $t_{d(OFF)}$  values. Without even knowing the  $t_{d(ON)}$  and  $t_{d(OFF)}$  for the MOSFET, the  $t_{rv}$  and  $t_{fv}$  in both tests are by themselves greater than the theoretical  $t_{ON}$  and  $t_{OFF}$  values. This could be due to multiple factors. The most likely reason for these differences is that the MOSFET simply isn't ideal. Actual MOSFETs can experience manufacturing deficiencies and degradation over time that causes them to act non ideally. Stray inductance is also a large issue in our board and could be causing performance issues. This is due to the MOSFET being placed too close to the low voltage portion of the PCB and causing EM disturbances as it switches. The inefficiencies are what leads to the actual circuit consuming more energy than theoretically calculated. The theoretical energy consumption is 9  $\mu\text{J}$  and 18  $\mu\text{J}$  for the  $I_D = 5 \text{ A}$  and  $10 \text{ A}$  tests respectively. The actual energy consumption is 8.73  $\mu\text{J}$  and 36.9  $\mu\text{J}$  for the  $I_D = 5 \text{ A}$  and  $10 \text{ A}$  tests respectively. The actual energy consumption in the 5 amp test is lower than the theoretical energy consumption which is impossible. This could be due to incorrect measurement of the turn on and off times along with using the theoretical values for part of the calculation. The actual energy consumption in the 10 A test is higher than the theoretical energy consumption which is expected. This could be due to any of the reasons previously stated, from deficiencies in the MOSFET's manufacturing to the high level of stray inductance in the circuit.

The boost converter configuration also experiences inefficiencies. In an ideal scenario, 100% of the input power would be consumed by the load with no loss in between. When calculating the theoretical efficiency of the system, however, several sources of loss such as the MOSFET and diode were taken into account. The theoretical efficiency was calculated as 85.33% and the actual efficiency of the system is 84.97%. These values are very close with the differences being explained by, as previously stated, a large stray inductance in the system along with components being even less ideal than assumed in the calculations.

This project illustrates the challenges of the PCB creation process, from design to manufacturing. It also illustrates that an error during any stage of the process can have implications on the performance of the circuit later on. This project helped us to acquire new skills such as PCB design and reflow soldering and taught us the level of detail required to efficiently and accurately analyze the performance of a power electronics circuit. The final performance of the circuit shows that there are several areas in which improvements can be made. Cleaner soldering would help to eliminate inconsistent connection issues that the PCB experienced and a smarter board layout would help to reduce the effect of the EMI generated by the MOSFET switching. Even with these deficiencies, however, this project was an overall success. We were able to successfully demonstrate DPT/Boost-Converter circuit and gained valuable insight into the process of circuit design and manufacturing for power electronics.

## **Summary**

In this project a custom PCB for MOSFET double pulse testing and a boost converter was designed and built from start to finish to. This process required learning a new PCB design software, Altium, and concepts related to the mechanics of power electronics PCB design, such as trace width and placement of EMI noisy components. Another big learning from this project was understanding how reflow soldering works and the difficulties that working with very small surface mount components can present. Lastly, this project then involved performing tests and

analysis on the PCB, illustrating the gap between ideal and actual performance, the many sources of failure in a single circuit, and the importance of attention to detail through the entire PCB creation process in order to maintain the circuit's integrity. One of the circuits designed for this project, the Double Pulse Test, is used as a method of testing the operating characteristics of switching devices, specifically MOSFETs. This PCB design experienced some deficiencies such as poor soldering joints and large stray inductance, but was able to successfully perform the DPT and also act as a boost converter. The circuit MOSFET was successfully analyzed through the DPT, where it was found that it acts less than ideally and generally has more energy losses than the theoretical case. The boost converter also acts less than ideally, operating at only 84.99% efficiency. This project instilled a deeper understanding of power electronics concepts as well as a broader knowledge of the engineering design process as a whole.

**Works Cited**

- [1] "Bluetooth controlled TRIAC DIMMER," Electronoobs. [Online].  
[https://electronoobs.com/eng\\_circuitos\\_tut20.php](https://electronoobs.com/eng_circuitos_tut20.php). Accessed Dec. 8, 2023.

## Appendices

### Appendix A: PCB Bill of Materials

Comment	Description	Designator	Footprint	LibRef	Quantity
C1206C104K5RAC TU	CAP, Ceramic, 0.1 uF, +/- 10%, 50 V, -55 to 125 degC, 1206 (3216 Metric), RoHS, Tape and Reel	C1, C2, C4, C6	KEMT-1206-2_M	CMP-1037-04202-2	4
CL31A225KB9LNN C	Cap Ceramic 2.2uF 50V X5R ±10% SMD 1206 +85°C Embossed T/R	C3, C16	FP-CL31-IPC_A	CMP-13271-003141-1	2
Samsung CL31A106KACLNN C	10 µF ±10% 25V Ceramic Capacitor X5R 1206 (3216 Metric)	C5, C17	CAPC3216X180X50ML20T25	CMP-20112613-2	2
10 uF	10 µF Film Capacitor - 500V Polypropylene (PP), Metallized Radial	C7, C8	DCP4_13.0WX24.0HX31.5L_2PIN_WIM	DCP4H151006DD2KSSD	2
220 nF	CAP CER 1812 220NF 500V X7R 10%, No Description Available	C9, C10, C11, C12, C13	CAPC480350_185N_KEM-M	C1812C224KCRACAUTO	5
Taiyo Yuden UMK316ABJ475K D-T	Cap Ceramic 4.7uF 50V X5R 10% SMD 1206 85°C Paper T/R	C14, C15	PCB-sgxvsk2a58hocmmem9zc-1	CMP-7a94b2a8e5e7a553-1	2
Würth Elektronik 885012207078	Capacitor, Mlcc, X7r, 1 uf, 25v, 0805	C18, C19	PCB-l1mgbkckj127aryzwzh1-1	CMP-e4702e9cfb553bb7-2	2
RFNL10BM6SFH	DIODE GEN PURP 600V 10A TO252	D1	RFNL10BM6SFH	RFNL10BM6SFH	1
LTL2R3KGD-EM	LED GREEN DIFFUSED T-1 3/4 T/H	D2	LTL2R3KGD-E	LTL2R3KGD-EM	1
Comchip CDBA240L-HF	DIODE SCHOTTKY 40V 2A DO214AC	D3	PCB-vqvgyl4w7md68ovtiswz	CMP-7a73b224736fa5b4-1	1
Keystone 575-4	Banana Jack, Non-Insulated, 1-Pin THD, RoHS, Bulk	J1, J2, J3	PCB-csc5n6emwyzdyne8ltju-1	CMP-d3511a5899970c96-2	3
691137710002	Series 1377 - 5.00 mm Horizontal	J4	69113771000	6911377100	1

	Entry with Pressure Clamp WR-TBL, 2 pin			2 02_1	
PJ-002AH-SMT-TR	Power Barrel Connector Jack 2.00mm ID (0.079"), 5.50mm OD (0.217") Surface Mount	J5	CUI-PJ-002AH- 4_V	CMP-2000-0 6896-1	1
TDK VLS252008ET-6R8 M	Ind Power Shielded Wirewound 6.8uH 20% 1MHz Ferrite 500A 1008 Blister Plastic T/R	L1	PCB-fkaygjadjj sdxx713cih-1	CMP-b1247 9fff73a6ee3 -1	1
Bourns SRF0905-100Y	Common Mode Chokes Dual 10uH 200Ohm 1kHz 1.6A 80mOhm DCR SMD T/R	L2	PCB-3xxuz9rz4 wogwyauw14r -1	CMP-726eb bfbaae1ada 9-1	1
IPD60R380C6	N-Channel CoolMOS C6 Power-Transistor, 600 V VDS, 10.6 A ID, -55 to 150 degC, PG-T0252-3-313, Reel, Green	Q1	INF-PG-T0252- 3-313_M	IPD60R380C 6	1
RMCF1206FT10K0	10 kOhms ±1% 0.25W, 1/4W Chip Resistor 1206 (3216 Metric) Automotive AEC-Q200 Thick Film	R1, R3	RESC3216X60 X45ML10T20	CMP-2003-0 1783-1	2
CRCW1206511RF KEA	510 Ohms ±5% 0.25W, 1/4W Chip Resistor 1206 (3216 Metric) Moisture Resistant Thick Film	R2	RESC3216X60 X45ML10T20	CMP-2003-0 2260-1	1
CRCW120612R0J NEA	RES SMD 12 OHM 5% 3/4W 1206	R4	RESC3216X60 X45ML10T20	CMP-2003-0 1783-1	1
CSRN2512FKR200	Res Thick Film 2512 0.2Ω 1% 2W ±200ppm/°C Molded SMD Plastic T/R	R5, R6	FP-CSRN2512- MFG	CMP-26527- 000009-2	2
RMCF1206FT1K00	1 kOhms ±1% 0.25W, 1/4W Chip Resistor 1206 (3216 Metric) Automotive AEC-Q200 Thick Film	R7	RESC3216X60 X45ML10T20	CMP-2003-0 1783-1	1
Keystone 5011	Test Point; Black; Thru-Hole; Snap-Fit; SilverPlate; 0.063in. Dia.; 0.445In.	TP2, TP5	PCB-qzb0vyxe bd51imkzt9uv- 1	CMP-399bf0 913da3e65c -1	2
ISO7710D	General Purpose Digital Isolator 3000Vrms 1 Channel 100Mbps 85kV/µs CMTI 8-SOIC (0.154", 3.90mm Width)	U1	D0008B_HV	ISO7710D	1
Texas Instruments	Single Inverting Buffer/Driver With	U2	PCB-kpbwuq3j	CMP-30e3f9	1

SN74LVC1G240DB VR	3-State Outputs 5-SOT-23 -40 to 125		jzqbef0a2xnc- 1	ef6642ef24- 3	
UCC27519DBVT	TEXAS INSTRUMENTS UCC27519DBVT DRIVER, GATE, 18VIN, 4A, NON-INV, 5SOT23	U3	PCB-2253518- 1	CMP-22535 18-3	1
CUI PDS1-S5-S12-M-T R	Isolated Module DC DC Converter 1 Output 12V --- 83mA 4.5V - 5.5V Input	U4	PCB-db6tqtrzp 4l61tosig05-1	CMP-0ec6c6 74b100d101 -1	1
STMicroelectronics LDK220M36R	LDK220 Series 2.5 to 13.2 Vin 200 mA 3.6 Vout LDO Linear Regulator - SOT23-5L	U5	SOT23-5L	CMP-5e1b9 542f71181d c-2	1

## Appendix B: Link for Selected Heatsink

DigiKey Product Link:

<https://www.digikey.com/en/products/detail/aavid-thermal-division-of-boyd-corporation/501100-B00000G/1625002>